Proceedings of the 17th World Congress
The International Federation of Automatic Control
Seoul, Korea, July 6-11, 2008

Modeling Neural Spiking Activity in the Sub-Thalamic Nucleus of Parkinson's Patients and Healthy Primates

Sridevi V. Sarma[1] Ming Cheng[2] Rollin Hu[2] Ziv Williams[2] Emery N. Brown[1,3] Emad Eskandar[2]

[1]*Massachusetts Institute of Technology, Cambridge, MA 02139 USA (Tel: 617-669-8933; e-mail:sree@ mit.edu).*
[2]*Al-Rohdan Laboratories – MGH-HMS Center for Nervous System Repair, Department of Neurosurgery, Massachusetts General Hospital, Boston, MA 02114.*
[3]*Neuroscience Statistics Research Laboratory, Department of Anesthesia and Critical Care, Massachusetts General Hospital, Boston, MA 02114.*

Abstract: How neurons in humans encode information about the outside world and how this processing changes when the brain is diseased are central questions in neuroscience and medicine. Historically, microelectrode recordings of single-unit neuronal activity have been confined to animal preparations. Recently, it has become possible to obtain single-unit recordings in humans undergoing deep brain stimulation surgery. In this study, we recorded neuronal activity from the sub-thalamic nucleus (STN) of the basal ganglia of patients with Parkinson's disease (PD). In parallel, identical experiments were conducted on a healthy primate, providing a rare opportunity to analyze STN neuronal activity recorded in both the disease and healthy state during the same behavioral tasks. We developed point process models of STN neurons to capture neural spiking dynamics as a function of extrinsic stimuli and the neuron's own spiking history. Our models quantify, for the first time, pathological signatures in PD neural activity such as bursting, 10-30Hz oscillations, and loss of directional plurality, which may directly relate to motor disorders observed in PD patients such as bradykinesia, resting tremor, and rigidity.

1. INTRODUCTION

An estimated 3-4 million people in the US have Parkinson's disease, a chronic and progressive neural disease that occurs when specific neurons in the midbrain degenerate, causing movement disorders such as resting tremor, rigidity, and bradykinesia (slowness in movement). Currently, there is no cure or treatment to stop disease progression. However, surgery and medications are available to relieve some of the symptoms short term, and perhaps even slow the progression of the disease. Such treatments for PD have been developed based on significant understanding of the basal ganglia (BG) anatomy and physiology (Albin et al., 1989).

It has been long appreciated that PD is caused when dopaminergic neurons degenerate in the substantia nigra pars compacta (SNc) in the midbrain. This triggers a cascade of functional changes in the BG which leads to hyperactivity of the BG output nuclei. Therefore all treatments try to reduce the hyperactivity by creating lesions in target areas, enhancing concentrations of dopamine in the SNc (via levodopa), or more recently by deep brain stimulation (Volkmann, 2007). DBS is a surgical procedure in which an electrode is inserted through a small opening in the skull and implanted in a targeted area in the BG (typically the subthalamic nucleus (STN)). The electrode is connected to another insulated wire (called the 'extension') that is passed under the skin of the head, neck and shoulder and terminated at the neurostimulator ('battery pack'). The neurostimulator, similar to a heart pacemaker, is as large as a silver dollar and typically sits under the collar bone. It delivers electrical stimulation to the tip of the electrode via the extension and blocks abnormal neural signals that cause tremor and other PD symptoms. The neurostimulator must be replaced via minor surgery every 3-5 years. See schematic of DBS system in Figure 1.

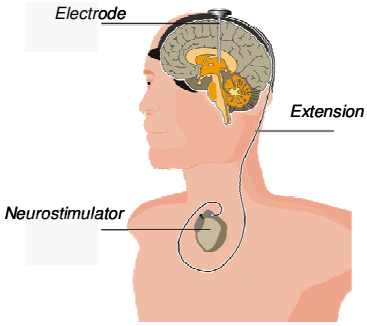

Fig. 1: Schematic of Deep Brain Stimulation System

While DBS is not a cure, it is perhaps the most effective treatment for improving quality of life for PD patients. DBS has also given neurophysiologists the rare opportunity to record neural activity in awake humans. During surgery, microelectrode recordings are routinely performed in order to confirm the location of the target nuclei. The need to record neural activity in order to confirm proper positioning of the microelectrode in the STN allows the study of neural activity in Parkinson's patients during movement at no additional risk

(Abosch et al., 2002; Arminovin et al., 2004; Arminovin et al., 2006). Therefore, we used the microelectrodes to record activity in the STN of PD patients executing a visual guidance task. For comparison, we conducted microelectrode recordings from the STN of healthy awake behaving primates executing the same task.

We analyze neural spiking activity of both Parkinson's patients and healthy primates using point process models (Truccolo et al., 2005). The models were fit to the STN neural spike trains using generalized linear model (GLM) methods (Brillinger et al. 1988; Truccolo et al. 2005). The point process paradigm is a probabilistic framework that is advantageous over traditional analyses which try to uncover intrinsic and extrinsic factors on neuronal spiking activity (mean firing rates, autocorrelation functions, inter-spike interval histograms, peri-stimulus time histograms, power spectra etc.) in that a single point process model (one computation) captures the relative contribution of short and long-term history effects (intrinsic factors) as well as the impact of movement direction (extrinsic factor) on the probability that the neuron will spike at any given time. The framework also allows us to assess model goodness-of-fit and construct confidence intervals for quantities of interest.

2. METHODS

Seven human subjects with Parkinson's disease were used in this study. The human subjects all had idiopathic PD for greater than 4 years, a Hoehn-Yahr score of 3 or higher and a documented response to levodopa replacement therapy. All patients had a pre-operative neurological exam with detailed information on their tremor and PD symptoms. Subjects were excluded from surgery if they had cognitive impairment, active psychiatric disorders, or anatomic abnormalities on magnetic resonance imaging. None of the patients had undergone prior surgery for the treatment of PD. Informed consent for participation in the study was obtained in accordance with a protocol approved by the Massachusetts General Hospital Institutional Review Board. The decision to perform surgery was made based on clinical indications and was not related to participation in this study. In all subjects, anti-Parkinsonian medications were withheld starting at midnight before the surgery. No sedatives were given during the surgery. The general techniques of stereotactic localization and intraoperative microelectrode recordings are described elsewhere (Amirnovin et al., 2004, 2006; Hutchison et al., 1998).

2.2 Primate Subject

One adult male rhesus monkey (macaca mulatta) was used in this study. A titanium head post, plastic recording chamber and scleral search coil were surgically implanted in accordance with guidelines set by the animal review committee at Massachusetts General Hospital. Neuronal activity was amplified, band-pass filtered between 200 Hz – 5 kHz, and sampled at 20 kHz. Spikes were stored and sorted off-line using a template-matching algorithm (Spike 2, Cambridge Electronics Design). Eye position and joystick position were each sampled and recorded at 1 kHz.elsewhere (Amirnovin et al, 2004, 2006; Hutchison et al, 1998).

2.3 Electrophysiological Recordings and Behavioral Task

Once the microelectrodes were in the STN, the subjects viewed a computer monitor and performed a behavioral task by moving a joystick with the contralateral hand. The joystick was mounted such that movements were in a horizontal orientation with the elbow flexed at approximately 45 degrees. The behavioural task consisted of two-stage paired trials. The first trial of each pair was denoted as "instructional" and began with the presentation of a small central fixation point. After a 500 ms delay, four small gray targets appeared arrayed in a circular fashion around the fixation point (Up, Right, Down and Left). After a 500-1000 ms delay a randomly selected target turned green (target cue) to indicate where the subject is to move. Then after another 500-1000 ms delay, the central fixation point turned green (go cue), cueing the subject to move. At this point the subject used the joystick to guide a cursor from the center of the monitor towards the green target. Once the target was reached, either a juice reward was given (in the primate case) or a tone sounded indicating the subject had successfully completed the task (human case), and the stimuli were erased. See Figure 3 for a schematic of an instructional trial. Subjects were required to return the joystick to the center position before the second trial of each pair started. The second trial of each pair was identical to its associated instructional trial in that the subject was required to move in the same direction. However, one or both of the cues could be omitted. Our analysis using second-stage trials are not presented here.

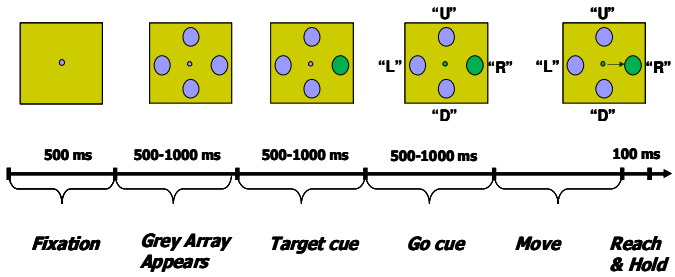

Fig. 3 Schematic of Task of Instructional Trial

2.4 A Point Process Model of STN Dynamics

We formulate a point process model to relate the spiking propensity of each STN neuron to factors associated with the trial types, movement direction, and features of the neuron's spiking history. Point process models have been shown to be useful in characterizing neural spiking activity (Brillinger, 1988, Barbieri et al., 2001, Kass and Ventura, 2001, Harris et al., 2003, Brown et al., 2001; Brown et al., 2003; Brown et al., 2005).

A point process is a binary stochastic process defined in continuous time (eg. number of neuronal spikes in a given time interval) and is characterized entirely by the conditional intensity function (CIF) which is defined below (Cox, 2000; Daley and Vere-Jones, 2003).

Consider the time interval $(0,T]$ as the continuum, and events as neuronal spike times. Let $t_1,...,t_n$ denote the times of each neural spike such that $0 < t_1 < t_2 ... < t_n \le T$ .Then, if $N(T)$ is the sample path of the associated counting process ($N(T)$ is the number of spikes in the interval $(0,T]$), the conditional intensity function is the following

$$\lambda(t \mid H_t) = \lim_{\Delta t \to 0} \frac{P(N(t+\Delta t) - N(t) = 1 \mid H_t)}{\Delta t}. \qquad (1)$$

H_t is the history of the sample path and that of any covariates up to time t , and $t_{N(t)}$ is the time of the last spike prior to t . Consequently,

$$\lambda(t \mid H_t)\Delta \approx \Pr ob(spike\ in\ (t, t+\Delta] \mid H_t). \qquad (2)$$

The well-known Poisson process is a special point process in which all events are independent and the CIF is constant and therefore not dependent on history. For this reason, we choose more general point process models, as is done in (Eden et al., 2007), instead of Poisson processes for our analyses.

To analyze the spiking propensity of the STN neurons, we define the CIF as a function of the movement direction which corresponds to "Up, Right, Left and Down"; and, the neuron's spiking history in the preceding 150 msec. We also divide time into before and after onset of a given epoch (e.g. movement) with the variable where if before onset and if after onset. Specifically,

$$\lambda(t \mid H_t, \theta) = \exp\left\{ \sum_{\ell=0}^{1} \left[\sum_{d=1}^{4} \alpha_{d,\ell} I_{d,\ell}(t) + \sum_{j=1}^{10} \beta_{j,\ell} n^{\ell}_{t-(j)t-(j+1)} + \sum_{k=1}^{14} \gamma_{k,\ell} n^{\ell}_{t-(10k+9)t-10k} \right] \right\} \qquad (3)$$

where the following quantities are computed from data: $I_{d,\ell}(t)$ is equal to 1 if movement is in direction d and time relative to onset is ℓ and equal to 0 otherwise; and, $n^{\ell}_{a:b}$ is the number of spikes observed in the time interval [illegible] for time relative to epoch onset ℓ .

The following comprise the model parameter vector $\theta = \{\alpha, \beta, \gamma\}$ to be fitted by data. The $\{\alpha_{d,\ell}\}$ parameters measure the effects of movement direction and time relative to epoch onset on the spiking probability, $\{\beta_{j,\ell}\}_{j=1}^{10}$ parameters measure the effects of spiking history in the previous 10 msec for a given time relative to onset and therefore, they capture the effects of refractoriness and bursting on the spiking probability, and $\{\gamma_{k,\ell}\}_{k=1}^{14}$ parameters measure the effects of the spiking history in the previous 10 to 150 msec for a given time relative to onset on the spiking probability, which may be associated with not only the neuron's individual spiking activity but also that of its local network. We built separate models for four different epochs. Specifically, we computed models for:

1. right after fixation point appears (FX+) : $t \in (0,350]$ ms
2. around target cue onset (TC-,TC+) : $t \in (-250,0]$ ms and $t \in (0, 250]$ ms
3. around go cue onset (GC-,GC+) : $t \in (-250,0]$ ms and $t \in (0, 250]$ ms
4. around movement onset (MV-,MV+) : $t \in (-250,0]$ ms and $t \in (0, 250]$ ms .

2.5 Model Fitting and Data Analysis

The model can be fit to the STN neural spike trains using GLM methods (Truccolo et al. 2005). The GLM is an extension of the multiple linear regression model in which the variable being predicted, in this case spike times, need not be Gaussian (McCullagh and Nelder, 1989). GLM provides an efficient computational scheme for model parameter estimation and a likelihood framework for conducting statistical inferences based on the estimated model (Brown et al., 2003).

We used Kolmogorov-Smirov (KS) plots based on the time-rescaling theorem to assess model goodness-of-fit. The time-rescaling theorem is a well known result in probability theory which states that any point process with an integrable conditional intensity function may be transformed into a Poisson process with unit rate (Brown et al. 2002; Truccolo et al. 2005). A KS plot, which plots the empirical cumulative distribution function of the transformed spike times versus the cumulative distribution function of a unit rate exponential, is used to visualize the goodness-of-fit for each model. The model is better if its corresponding KS plot lies on the 45 degree line. We computed 95% confidence bounds for the degree of agreement using the distribution of the KS statistic (Johnson and Kotz, 1970).

We note that we first discretized time by partitioning the time interval into 1 msec bins and estimated the discretized CIF. Finally, we computed maximum-likelihood estimates and confidence intervals of for each neuron using glmfit.m in MATLAB.

In this paper, we focus on the following global hypothesis: H1: The neural spiking activity in the STN is different in healthy primates and in Parkinson's patients.

3. RESULTS

As mentioned above, we built point process models for several neurons for 4 different epochs using PD and primate data. For the PD instructional trial data, 29 models passed the KS-test in that each KS plot lied within the 95% confidence bounds. For the primate data, 44 models passed the KS-test. This indicates that the 29 point process models

fit the PD data well while 44 point process models fit the primate data well.

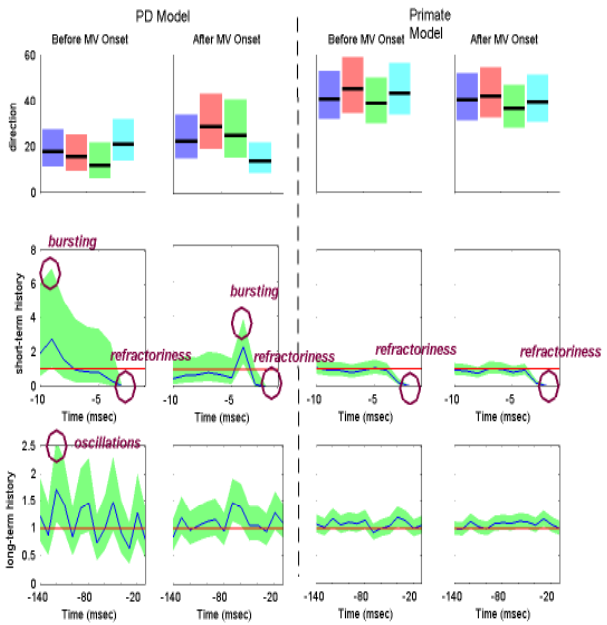

Fig. 3: Optimal model parameters for an STN neuron during MV- and MV+ periods of a PD patient (left) and healthy primate (right) during IT Trials. Top row (movement direction modulation): optimal extrinsic factors $e^{\alpha_{d,l}}$ for d=U,R,D,L and l=before and after movement onset are plotted in black lines and corresponding 95% confidence intervals are shaded around each black line in a unique color for each direction. Middle row (short-term history modulation) optimal short-term history factors e^{β_i} for i=1,2,…,10 are plotted in blue and corresponding 95% confidence intervals are shaded in green. Bottom row (long-term history modulation) optimal long-term history factors e^{γ_j} for j=1,2,…,14 are plotted in blue and corresponding 95% confidence intervals are shaded in green.

Recall from equation (2) that $\lambda(t \mid H_t)\cdot\Delta$ is approximately the probability that the neuron will fire at time t given extrinsic and intrinsic dynamics up to time t, which is captured in H_t. By virtue of equation (3), we allow the probability that each STN neuron will fire at some time t to be modulated by movement direction, short-term history and long-term history spiking dynamics. Figure 3 illustrates these three modulation factors on spiking activity for both PD and primate single neuron models by plotting the optimal parameters and their corresponding 95% confidence bounds before and after movement onset. We make the following observations:

1. **Refractoriness:** As illustrated in the second row of Figure 3, both the PD and primate STN neurons exhibit refractory periods before and after onset of movement as indicated by down modulation by a factor of 10 or more due to a spike occurring 1 msec prior to a given time t. That is, if a spike occurs 1 msec prior to time t, then it is very unlikely that another spike will occur at time t ($e^{\beta_1} \le 0.1$ for all e^{β_1} within its 95% confidence band). This is expected since after an action potential (a spike) occurs, some time (refractory period) must elapse before the neuron can again produce another action potential in response to a stimulus (Brodal, 1998).

2. **Bursting:** As illustrated in the second row first two columns of Figure 3, the PD neuron fires in rapid succession before and after movement onset as indicated by up modulation by a factor of 2 or more due to prevalent spiking activity occurring 2-10 msec prior to some time t. That is, if a spike occurs 2-10 msec prior to time t, then it is very likely that another spike will occur at time t ($\max(e^{\beta_2}, e^{\beta_3}, \ldots, e^{\beta_{10}}) \ge 2$ for any e^{β_i} within its corresponding 95% confidence band for i=2,3,…,10). In contrast the primate neuron model shown in Figure 3 does not exhibit any bursting and is not modulated much by short or long-term history.

3. **10-30 Hz Oscillations:** As illustrated in the third row first two columns of Figure 3, the PD STN neuron exhibits10-30 Hz oscillatory firing before and after movement. That is, the probability that the PD STN neuron will fire at a given time t is up modulated by a factor of 2 or more if a spike occurs 30-100 msec prior to t ($\max(e^{\gamma_2}, e^{\gamma_3}, \ldots, e^{\gamma_{10}}) \ge 2$ any within e^{γ_i} its corresponding 95% confidence band for i=2,3,…,10).

4. **Directional Selectivity:** As illustrated in the first row of Figure 3, the PD STN neuron appears to exhibit more directional selectivity before and after movement onset than the primate neuron. That is, the PD neuron seems more likely to fire in some directions than in others unlike the primate neuron. To quantify directional selectivity, we performed the following test for each neuron and each time relative to onset (ℓ):

1. For each direction $d^* = \{U, R, D, L\}$, compute $p_{d^*,d} = \text{Prob}(e^{\alpha_{d^*,l}} > e^{\alpha_{d,l}}) = \text{Prob}(\alpha_{d^*,l} > \alpha_{d,l})$ for $d \ne d^*$. Define $p_{d^*,d^*} = 0$. Use the Gaussian approximation for $\alpha_{d,l}$, which is one of the asymptotic properties of ML estimates to compute $p_{d^*,d}$ (Brown et al., 2003).

2. If $\max_{d^*=1,2,3,4} p_{d^*,d} \ge 0.8$ then neuron exhibits directional selectivity.

Table 1. STN Neural Activity Characteristics of PD (top) and Primate (bottom) Models.

Characteristic	**Epochs (% from 29 PD neuron models)**							
	FX+	**TC-**	**TC +**	**GC-**	**GC +**	**MV -**	**MV +**	**(-,+) Avg**
Refractoriness	100	100	100	100	100	100	100	(100, 100)
Bursting	76	93	76	90	76	79	69	(87, 74)
10-30 Hz Oscillations	76	93	41	90	38	79	31	(87, 37)
Directional Selectivity	7	14	21	10	10	24	41	(16, 24)
Characteristic	**Epochs (% from 44 primate neuron models)**							
	FX+	**TC-**	**TC +**	**GC-**	**GC +**	**MV -**	**MV +**	**(-,+) Avg**
Refractoriness	98	98	95	98	98	98	93	(98, 95)
Bursting	11	14	9	18	8	16	9	(16, 9)
10-30 Hz Oscillations	11	14	2	18	7	16	5	(16, 5)
Directional Selectivity	0	2	5	0	0	5	11	(2, 5)

We make the following observations from Table 1 with regards to neural spiking activity in the STN of PD patients and primates during instructional trials. Most or all neurons in both species exhibit refractoriness. Bursting is prevalent across all epochs modeled in neural activity of PD patients (69% or more PD neurons burst). In contrast, neural activity in the healthy primate exhibits little bursting (18% or less) across all epochs. In both species, bursting decreases after the onset of a visual or movement stimulus. 10-30 Hz oscillations are prevalent in neural activity of PD patients right before the onset of visual cues (90% or more PD neurons oscillate before a visual cue is shown) or movement onset (79%). In contrast, neural activity in the healthy primate exhibits little oscillation (less than 18%) before visual stimuli and only 16% of the primate neurons modeled oscillate before movement onset. 10-30Hz oscillations in neural activity for both species decrease by more than 50% after the onset of either a visual cue or movement. Overall directional selectivity is more prevalent in PD neurons (7 - 41%) than in primate neurons (0 -11%). Directional selectivity is insignificant during fixation or during the go cue epoch for either diseased or healthy subjects. More directional selectivity appears during target cue and movement epochs, and increases with the onset of each epoch (by 50%-70% in PD neurons and 120%-150% in primate neurons). In both primate and PD neural activity, there are significant differences in the intrinsic properties right before the onset of a stimulus (visual or behavioral) to those right after the onset of a stimulus. In particular, bursting and oscillations decrease after onset of a stimulus while directional selectivity increases with the onset of a stimulus.

4. DISCUSSION

Prior to this study, characterizations of STN neural activity in PD patients were being quantified without comparisons to healthy STN neurons (Williams et al., 2004; Amirnovin et al., 2004; U.T. Eden, J. Gale, R. Amirnovin, E.N. Brown, E. Eskandar, unpublished observations). In this paper, we employ a rigorous point process modeling framework to quantify differences in STN neural activity between healthy primate subjects and human PD patients under identical experimental conditions.

In support of our global hypothesis that neural spiking activity in the STN is different in healthy primates and in PD patients, we found that neural activity of PD patients exhibits significantly more bursting, 10-30 Hz oscillations and greater directional selectivity than the healthy primate. These neurophysiological characteristics may explain some of the motor disorders observed in Parkinson's patients.

The bursting activity or sudden rapid succession of spikes indicates abnormal firing patterns in the STN associated with disease, which may be blocking important information about the subject's intent to move from being processed appropriately in the basal ganglia or from being relayed properly in the thalamus causing rigidity and bradykinesia. Bursting in STN activity of PD patients has previously been observed (Bergman et al 1994; Levy et al., 2001; U.T. Eden, J. Gale, R. Amirnovin, E.N. Brown, E. Eskandar, unpublished observations) and is consistent with simulations generated from a conductance-based biophysical model of the Parkinsonian STN developed by Rubin and Terman (2004).

The 10-30 Hz oscillations in STN neural activity may relate to the resting tremor which typically is observed to be on the order of 3-6Hz (Dostrovsky and Bergman, 2004; Vaillancourt and Newell, 2000). Such oscillations have been observed in Parkinsonian green monkeys (Bergman et al., 1994) and in PD patients undergoing functional stereotactic mapping (Levy et al., 2002). In the latter study, patients with limb tremor showed significant synchronized oscillations in the STN whereas patients without limb tremor did not, suggesting that 10-30Hz oscillatory activity may be associated with the pathology that gives rise to tremor in PD patients. However, in Amirnovin et al. (2004), the 10-30 Hz oscillations observed in the STN of PD patients undergoing DBS neurosurgery were not correlated with observed resting tremor in the patients. These differences in observations may be due to variability between patients, the dynamic nature of tremor or differences in task conditions.

Perhaps our most surprising finding is that directional selectivity in the STN increases in the disease state. Previous studies show context-dependent modulation of neuronal activity in the STN and the internal segment of the globus pallidus in both healthy primates and PD patients (Georgopoulos et al., 1983; Gdowski et al., 2001; Abosch et

al., 2003; Paradiso et al., 2003; Turner and Anderson, 2005). Although there seems to be more studies on healthy primates that show movement-related modulation in these deep nuclei, it is unclear how such modulation in healthy subjects compares to that in PD subjects. One may argue that movement direction and other specific details are represented in the higher motor cortical areas (Rickert et al., 2005) and that the deep nuclei of the BG in healthy subjects should have little directional selectivity and only process information about general movement preparation. Thus, increased directional selectivity in STN neurons in the disease state can be interpreted as less directional plurality in that the STN neurons respond less to some or all target directions; and, that this may be the cause for slowness of movements or inability to initiate movements as is observed in many PD patients. This remains to be investigated with further comparison studies.

REFERENCES

Abosch A, Hutchison WD, Saint-Cyr JA, Dostrovsky JO and Lozano AM (2002) Movement-related neurons of the subthalamic nucleus in patients with Parkinson disease. J Neurosurg 97: 1167-1172

Albin RL, Young AB, Penney JB (1989) The functional anatomy of basal ganglia disorders. Trends Neurosci 12:366–375

Amirnovin R, Williams ZM, Cosgrove GR & Eskandar EN (2004) Visually guided movements suppress subthalamic oscillations in Parkinson's disease patients. J. Neurosci. 24(50):11302-11306.

Amimovin R, Williams ZM, Cosgrove GR, Eskandar EN (2006) Experience with microelectrode guided subthalamic nucleus deep brain stimulation. Neurosurgery. Feb;58(1 Suppl):ONS96-102.

Barbieri R, Quirk MC, Frank LM, Wilson MA, and Brown EN (2001). Construction and analysis of non-Poisson stimulus response models of neural spike train activity. J Neurosci Methods 105: 25-37, 2001.

Bergman H, Wichman T, Karmon B, DeLong MR (1994) The primate subthalamic nucleus. II. Neuronal activity in the MPTP model of parkinsonism. J Neurophysiol 72:507–520

Brodal Per. (1998) The Central Nervous System: Structure and Function. Oxford Univ. Press, New York.

Brown EN, Nguyen DP, Frank LM, Wilson MA, Solo V. (2001) An analysis of neural receptive field dynamics by point process adaptive filtering. Proc Natl Acad Sci USA 98:12261-12266.

Brown EN, Barbieri R, Ventura V, Kass RE, and Frank LM. (2002) The time-rescaling theorem and its application to neural spike train data analysis. Neural Comput 14: 325-346.

Brown EN, Barbieri R, Eden UT, and Frank LM. (2003) Likelihood methods for neural data analysis. In: Feng J, ed. Computational Neuroscience: A Comprehensive Approach. London: CRC, Chapter 9: 253-286.

Brown EN. (2005) Theory of Point Processes for Neural Systems. In: Chow CC, Gutkin B, Hansel D, Meunier C, Dalibard J, eds. Methods and Models in Neurophysics. Paris, Elsevier; Chapter 14, pp. 691-726.

Cheng ML, Hadar E, Murrow R. (2006) Active Contact Location of Patients on Minimal or no Medication for Parkinson's Disease after STN DBS placement. ASSFN Abstract, Boston.

Cox DR, Isham V. (2000) Point Processes. Boca Raton, FL: CRC.

Daley D and Vere-Jones D. (2003) An Introduction to the Theory of Point Process. 2nd ed., Springer-Verlag, New York.

Dostrovsky J, Bergman H (2004) Oscillatory activity in the basal ganglia—relationship to normal physiology and pathophysiology. Brain 127:721–722.

Eden UT, Frank LM, Barbieri R, Solo V, and Brown EN. (2004) Dynamic analysis of neural encoding by point process adaptive filtering. Neural Comput 16: 971-998.

Gdowski MJ, Miller LE, Parrish T, Nenonene EK, Houk JC. (2001) Context dependency in the globus pallidus internal segment during targeted arm movements. J Neurophysiol. Feb;85(2):998-1004.

Georgopoulos AP, DeLong MR, Crutcher MD (1983) Relations between parameters of step-tracking movements and single cell discharge in the gobus pallidus and subthalamic nucleus of the behaving monkey. J Neurosci 3: 1586-1598.

Harris KD, Csicsvari,J, Hirase H, Dragoi G, Buzsaki G. (2003) Organizations of cell assemblies in the hippocampus. Nature, Vol 424, July.

Hutchison WD, Dostrovsky JO, Walters JR, Courtemanche R, Boraud T, Goldberg J, and Brown P. (1994). Neuronal Oscillations in the Basal Ganglia and Movement Disorders: Evidence from Whole Animal and Human Recordings. The Journal of Neuroscience. 24(42): 9240-9243.

Hutchison WD, Allan RJ, Opitz H, Levy R, Dostrovsky JO, Lang AE, Lozano AM (1998) Neurophysiological identification of the subthalamic nucleus in surgery for Parkinson's disease. Ann Neurol 44(4):622-8.

Kass RE and Ventura V. (2001) A spike train probability model. Neural Comput 13: 1713-1720.

Levy R, Dostrovsky JO, Lang AE, Sime E, Hutchison WD, and Lozano, AM. (2001) Effects of Apomorphine on Subthalamic Nucleus and Globus Pallidus Internus Neurons in Patients With Parkinson's Disease. J Neurophys. 86, 249-260.

Levy R. et al (2002) Dependence of subthalamic nucleus oscillations on movement and dopamine in Parkinson's disease. Brain 125, 1196-1209.

McCullagh P and Nelder JA. (1989) Generalized Linear Models (2nd ed.). Boca Raton, FL: Chapman & Hall/CRC.

Paradiso G, Saint-Cyr JA, Lozano AM, Lang AE, Chen R. (2003) Involvement of the human subthalamic nucleus in movement preparation. Neurology, 61(11):1538-45.

Rickert J, Cardoso de Oliveira S, Vaadia E, Aertsen A, Rotter S, Mehring C. (2005) Encoding of Movement Direction in Different Frequency Ranges of Motor Cortical Local Field Potentials. J. Neurosci., 25: 8815 - 8824.

Rubin J, Terman D. (2004) High Frequency Stimulation of the Subthalamic Nucleus Eliminates Pathological Thalamic Rhythmicity in a Computational Model. J. of Computational Neuroscience 16, 211-235.

Turner RS, Anderson ME. (2005) Context-dependent modulation of movement-related discharge in the primate globus pallidus. J Neurosci. Mar 16;25(11):2965-76.

Truccolo W, Eden UT, Fellow MR, Donoghue JP, and Brown EN (2005). A point process framework for relating neural spiking activity for spiking history, neural ensemble and extrinsic covariate effects. J Neurophys 93: 1074-1089.

Vaillancourt DE, Newell KM. (2000). The dynamics of resting and postural tremor in Parkinson's disease. Clin Neurophysiol. Nov;111(11):2046-56.

Volkmann J. (2007) Update on surgery for Parkinson's disease. Curr Opin Neurol. Aug; 20(4):465-9.

Williams ZM, Neimat JS, Cosgrove GR, Eskandar EN. (2005) Timing and direction selectivity of subthalamic and pallidal neurons in patients with Parkinson disease. Exp Brain Res. May; 162(4): 407-416.